



Expression and function of VEGFRs in normal epidermis and psoriatic lesional keratinocytes

Yong Wang^{1*}, Yong Yan², Huiwen Yu², Guangrong Jiang³, Shiyong Zhao², Meng Yi²

¹ School of Medicine, Yichun University, Yichun, 336000, China

² Department of Dermatology, Yichun People's Hospital, Yichun, 336000, China

³ Department of Clinical Laboratory, Yichun People's Hospital, Yichun, 336000, China

ARTICLE INFO

Original paper

Article history:

Received: April 01, 2023

Accepted: August 05, 2023

Published: August 31, 2023

Keywords:

Keratinocytes, Normal epidermis, Psoriasis, VEGFRs

ABSTRACT

The study aimed to explore the expression and function of VEGFRs in normal epidermis and keratinocytes of psoriatic lesions. In this study, the expression and role of VEGFRs in keratinocytes were examined using examples from psoriatic and healthy individuals. The experiment was completed by immunofluorescence analysis, reverse transcription polymerase chain reaction, Western blot, and real-time quantitative RT-PCR after the skin of nonlesional, adjacent, and lesional skin was excised. Observations indicated that in non-lesional psoriatic areas and adjacent lesional areas of the skin of psoriasis patients, the fluorescent signals of VEGFR-1 and VEGFR-2 were strongly labelled with keratinocytes, and in psoriatic lesions, keratinocytes were present throughout the entire thickness of the epidermis, with the exception of the stratum corneum. The distribution of VEGFR-3 in psoriatic nonlesional and adjacent lesional skin was consistent with that in normal epidermis, whereas all layers of the epidermis of psoriatic lesions expressed VEGFR-3. The mRNA expression levels of VEGFR-1,2,3 steadily increased from the normal epidermis to the psoriatic nonlesional, adjacent lesional, and perilesional areas, with the lesional epidermis' keratinocytes exhibiting the greatest levels of mRNA expression. Ca ions upregulate VEGFR-1,2,3 mRNA and protein expression in keratinocytes of nonlesional areas of psoriasis. VEGFRs protein expression and cortical IOD values of psoriatic and normal population cells showed a positive correlation. Hence, in comparison to normal epidermal keratinocytes, psoriatic lesional regions' keratinocytes considerably enhanced their expression of VEGFR-1,2,3 mRNA and protein. The overexpression of VEGFR-1,2,3 in psoriatic lesions may be encouraged by VEGF and Ca²⁺ ions.

Doi: <http://dx.doi.org/10.14715/cmb/2023.69.8.8>

Copyright: © 2023 by the C.M.B. Association. All rights reserved.

Introduction

The expression of VEGFR-1,2,3(V1, V2, V3) mRNA and protein by keratinocytes in psoriatic lesional regions was significantly higher than that of normal epidermal keratinocytes, with clinical features including dermal vascular changes, lymphocytic infiltration, abnormal differentiation and hyperproliferation of epidermal keratinocytes. Angiogenesis is essential to the growth of psoriasis under both healthy and pathological circumstances, according to recent studies. And angiogenesis is the most important biological process, which is influenced by growth factors and related intravascular growth factors (VEGF) and counterpart receptors (VEGFRs). Nrp-2 and neuropilin (NRP)-1 are the coreceptors for the VEGFRs, which comprise VEGFR-1, 2, and 3. VEGFR-1 expression is localized to vascular endothelial cells and part of nonvascular endothelial cells, and in early developmental stages, it is a negative regulator of angiogenesis. But in pathological conditions, it can promote angiogenesis (1-3). VEGFR-2 expression is mainly located in lymphatic and vascular endothelial cells, where it can promote cell mitosis and angiogenesis, as well as being an important mediator of hyperpermeability effects. V3 activation and lymphangiogenesis are tightly linked, with endothelial cells lining

the lymphatic vasculature at the early stages of development and staying in the lymphatic endothelium until the organ matures. The molecular weight of NRP-1, a cell surface glycoprotein that shares 44% of the sequence with NRP-2, is 130–140 kDa. All NRP-1 is expressed in the skeletal, cardiovascular, and nervous systems during embryonic development, and in the adult, it can be expressed in bone marrow stromal cells, osteoblasts, pancreas, kidney, liver, heart, lung, tumor cells, endothelial cells (4-6). However, there is still no wide recognition of the etiology and pathogenesis of psoriasis, meanwhile, the association of epidermal keratinocyte biological behavior and VEGFR is unprompted, and the study conducted an in-depth analysis to further elucidate the updated mechanism of the psoriatic epidermis.

Materials and Methods

General information

The inclusion criteria for those suffering from chronic plaque-type psoriasis (moderate to severe) from our hospital's outpatient or inpatient dermatology department can be attributed to three factors ① The diagnosis is confirmed by both pathological examination and clinical findings, ② Patients had not used any medication prior to sampling

* Corresponding author. Email: wylcy666@163.com

The selected areas of the specimens were skin, adjacent lesional skin, and nonlesional skin. The exclusion criteria can be attributed to the following three points. ① A in the minor Did not sign the informed consent form; ③ No severe heart, kidney and other diseases. Meanwhile, normal healthy adult skin from the Department of Orthopedics and Dermatology was studied, and the subcutaneous adipose tissue was cut and divided into two parts, which were placed in liquid nitrogen and % disease.

Research methods

Immunofluorometric assay

In flasks (25 cm² culture), normal epidermal keratinocytes, psoriatic nonlesional, and lesional epidermal keratinocytes neighboring were seeded. The coverslips were then passed through an incubation process and treated with 50% h2s04 overnight at 37 °C in 5% CO₂. All four samples were cut to a thickness of 4 μm by a Leica cm 1850 freezing microtome and transferred to coverslips. Using a solution containing sodium citrate (10 mm), cells were heated (20 minutes at 95°C) after being fixed with 3.4% paraformaldehyde for 20 min at room temperature. The washing was completed again by utilizing phosphate buffer solution in the same way, and at room temperature, the membrane was penetrated by 0.1% triton-100 in phosphate buffer for 15 min. Then they were blocked using 10% rabbit serum for 1 h at room temperature, and 20 UG/ml VEGFR-1,2,3 were added dropwise to different coverslips and washed again using the same method. A fluorescein isothiocyanate labeled Rabbit anti-mouse secondary antibody (1:40) was incubated in the dark (room temperature for 2h). And then conduct another wash done with the same method, counterstained with propidium iodide (PI) in the dark for 20 min, and observed and photographed under a fluorescence microscope to record the cumulative optical density value (integrated optical density, IOD).

RT-PCR

Reverse transcription polymerase chain reaction (RT-PCR) involves primer design and synthesis, extraction of non-deoxyribonucleic acid (RNA), reverse transcription, PCR reaction, electrophoresis, and sequencing. Experiments primers were designed by deoxyribonucleic acid (DNA) star software and Table 1 refers to PCR primer sequences.

20 l reverse transcription system reverse transcribed 2μg of extracted total RNA into cDNA (Invitrogen), 20u RNase inhibitor, 200u reverse transcriptase at 42°C for 60min and then stored at - 20°C after heat inactivation of reverse transcriptase at 95°C for 10min. The PCR reaction system was 25μ L and consisted of 10pmol of each pair of up - and downstream primers, 200mmol/LD ribonucleotide triphosphate mix, 2.5mmol/lmgck2, ph8.3 10mmol/L Tris HCl, 50mmol/lkcl, 2utaq enzyme, 1μ l cDNA, diethylpyrocarbonate water to make up to 25μ L. The reaction program was as follows: 1 cycle at 96°C temperature for 3 min. A total of 35 cycles were run for 1 min at 72°C, 1 min at 57°C, and 1 min at 96°C. Negative controls were reverse transcribed samples without reverse transcriptase to avoid amplification of contaminating genomic DNA. The gene expression internal reference was glyceraldehyde-3-phosphate dehydrogenase (GAPDH) with an annealing temperature of 55°C. The reaction products were electrophoresed in a 1.5% agarose gel containing a

certain amount of ethidium bromide, the recording instrument was a gel imager, and the sequencing of the products was all done by Shanghai SANGON company.

Quantitative real-time RT-PCR

Real-time PCR was used in the experiments to quantitatively evaluate the levels of gene expression, including reaction system, standard curve, reaction conditions, and data acquisition and calculation. The standard curve refers to dividing the sample cDNA according to ×4, ×16, ×64, ×256-fold specific dilution, and then the crossing point (CP) CP value was obtained to plot the standard curve. Two replicate reactions were set up for all reactions, while a blank control without a template was set up for each reaction. The CP value of the target gene and GAPDH Gene, and the CP value of the diluted template were entered in Qbase version 1.3.5 software, according to the instructions to obtain the relative internal control gene GAPDH expression level of the target gene.

Western blot assay

Western blot assays include the preparation of protein samples, determination of protein content, electrophoresis, membrane rotation, immunoreaction, and development operations. Each flask of cells should have 3 ml of 4°C precooled phosphate buffer solution added to it. Cells should then be gently rocked for 1 minute while being washed, and the wash should then be discarded. Repeat the process twice more for a total of three washes to clear the broth. Add 300μ l of ice-cold lysis solution and proceed to lysis for 30min, scrape the cells by scraping the side of the culture solution. The lysate and cell debris were next moved to a 1.5 ml centrifuge tube, which was operated by centrifugation at 12000 rpm for 10 min in a 4 °C environment. Then 20 μ l of the centrifuged supernatant was taken for protein quantification, and the rest was transferred to a 0.5ml centrifuge tube and an equal amount of 2 × loading buffer, boiled for 5-10 min and put in -80°C storage temperature. After the quantification was completed by bicinchoninic acid (BCA) protein assay kit, the cells were boiled in a dry bath pot at 100°C for 10 min and placed at - 20 °C for further use. Studies used sodium dodecyl sulfate-polyacrylamide gel electrophoresis with electrophoresis run in accordance with the configured sample size. The sample protein of each well on the glue was reducing agent buffer + sample buffer + target protein + secondary distilled water for a total of 30 UG / UL, which was placed in a 75°C constant temperature water bath and heated for 10 min. Place on ice to be loaded after vortexing for 10s, remove 12 well bis tris nupage gel in a 4°C cold room and subsequently add protein samples to wells on BIS tris nupage gel. The voltage intensity was set to 170V and the time was 70 min for electrophoresis. Transmembrane solution 20ml nupage buffer + 20ml methanol + 360ml secondary distilled water. The polyvinylidene difluoride membrane was activated by methanol immersion for 10 s, and after the completion of electrophoresis, the BIS tris nupage gel was carefully removed and attached with the polyvinylidene difluoride membrane, and the two ends were wrapped into sponges and filter paper and stuck into the transmembrane cassette. Throughout the primary and secondary antibody incubation stages, great attention is paid to ensuring that the incubation period for the secondary antibody is not excessively long. Image analysis software Image Lab was

used to process the images.

VEGFRs and VEGF expression

In these experiments, the impact of VEGF on the interpretation of VEGFRs in keratinocytes isolated from nonlesional areas of psoriasis was examined using 10 ng/ml VEGF165 as an example, and the effect of VEGF on the expression of VEGFRs was examined using bevacizumab, a specific neutralizing monoclonal antibody to VEGF. Confluent psoriatic nonlesional region keratinocytes were treated with 0, 0.5, 1.0, 2.0, and 3.0 mm CaCl₂ in specified keratinocyte serum-free media in a 5% CO₂ environment (37°C, 24 hours) to extract total RNA and protein. RNA was reverse transcribed to cDNA and proteins were separated by electrophoresis.

Statistical methods

The mean and standard deviation of the measurements, which had a normal distribution, were used to compare two groups and one-way ANOVA was used to compare several groups. The method of analysis of variance between groups was a non-parametric test *Z* if they did not follow a normal distribution, in which case they were stated using quartiles. The Kruskal-Wallis test was used to compare data between groups. Count data were expressed as columns or percentages, and the test was the χ^2 test. Bivariate normally distributed data were analysed using Pearson correlation coefficient analysis and non-normally distributed data were analysed using Spearman correlation coefficient analysis. Data comparisons were considered statistically significant when $p < 0.05$.

Results

Immunofluorescence localization analysis

The results of immunofluorescence localization of VEGFRs on psoriatic keratinocytes and normal skin keratinocytes are shown in Figure 1. Green fluorescence refers to VEGFRs expression and red fluorescence refers to PI counterstaining nucleus. The psoriatic lesional epidermis is hyperkeratotic and parakeratotic with hypertrophy of the stratum spinosum, elongation of the epidermal processes, and prominent angiogenesis and vascularization. The epidermal thickness of the neighboring psoriatic lesion region was noticeably thinner compared to the psoriatic lesion area. However, the epidermis of nonlesional areas was further thinned, which was almost the same thickness as that of a normal human epidermis, and only a few fine capillaries were found in the papillary layer of normal human dermis. Keratinocyte VEGFRs in normal epidermis and nonlesional areas of psoriasis are predominantly membranous in distribution, whereas keratinocyte VEGFRs in adjacent nonlesional and perilesional areas of psoriasis are found on the cell membrane and cytoplasmic membrane.

RT-PCR detection of VEGFRs expression

The expression profiles of VEGFRs detected by RT-PCR are shown in Figure 2. The amplified cDNA of *nrp-2*, *vegfr-3*, *NRP-1*, and *VEGFR-1,2* from normal epidermis and psoriatic lesion cells was 655 BP, 614 BP, 346 BP, 441 BP, and 436 BP, respectively, the sequence of which was identical to that given in GenBank, while there were no bands in the negative set.

Results of RNART-PCR for VEGFRs in vitro

Figure 3 (a) refers to the Western blot detection results of VEGFRs. The mRNA of VEGFRs in psoriatic patients showed various degrees of expression, however, the expression levels increased gradually from the normal epidermis to psoriatic nonlesional, adjacent lesional, and perilesional areas, and the highest expression level was observed in keratinocytes of the lesional epidermis. Figure 3 (b) refers to the scatter plot of band density ratios of VEGFRs to GAPDH. The mRNA expression of VEGFRs in keratinocytes of the psoriatic lesion area was dissimilar from that of cells in some other groups ($P < 0.001$).

Figure 4 refers to the four cellular VEGF mRNA expression levels in real-time fluorescence relative to quantitative PCR results. Relative to normal epidermal keratinocytes, the level of expression in psoriatic keratinocytes was statistically significant ($P < 0.001$).

Results of mRNART-PCR of VEGFRs cultured in vivo

Figure 5 (a) refers to the Western blot detection results

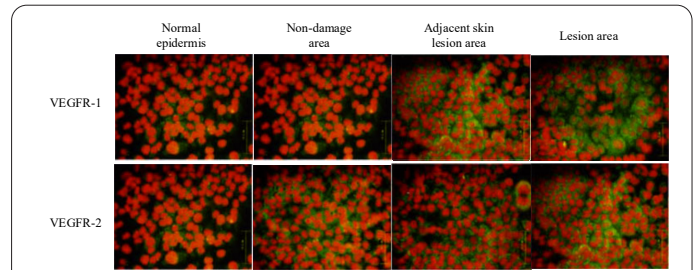


Figure 1. Immunofluorescence localization results (Ruler:50µm).

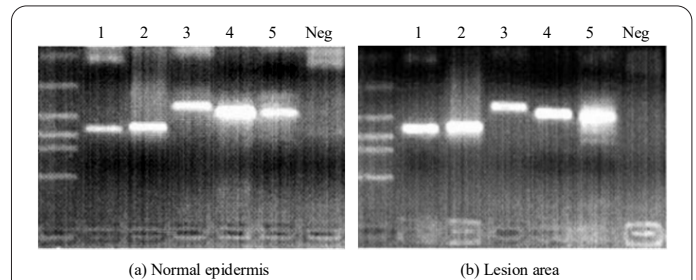


Figure 2. Detection of VEGFRs expression by RT-PCR.

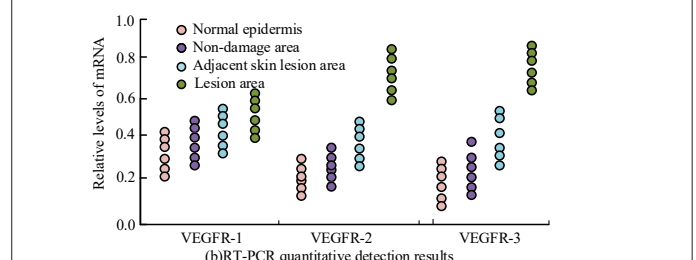
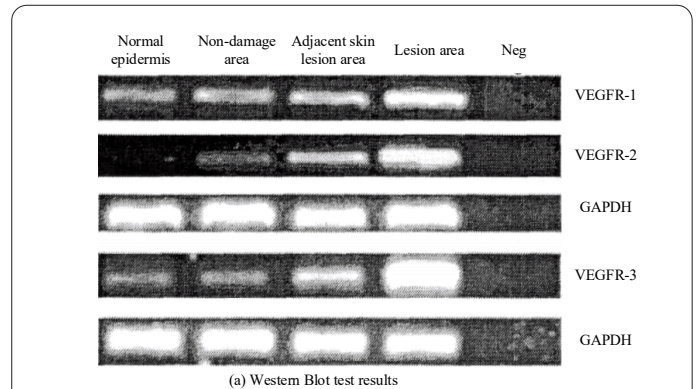


Figure 3. MRNART-PCR results of VEGFRs cultured in vitro.

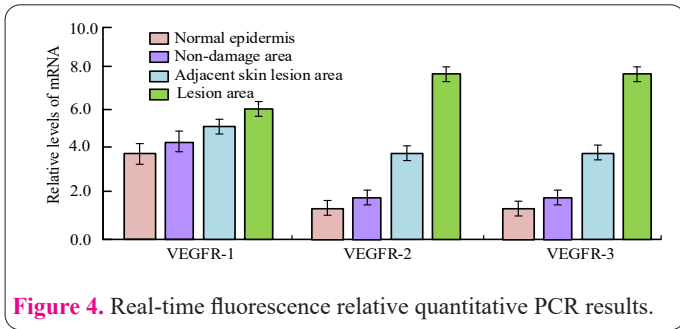


Figure 4. Real-time fluorescence relative quantitative PCR results.

of VEGFRs. The mRNA of VEGFRs in psoriasis patients all showed different degrees. Figure 5 (b) refers to the scatter plot of band density ratios of VEGFRs to GAPDH. The mRNA expression of VEGFRs in keratinocytes of the psoriatic lesion area was significantly different from that of cells in other groups ($P < 0.001$).

Effect of Ca ions on VEGF in keratinocytes of nonlesional areas of psoriasis

Figure 6 (a) refers to the scatter plot of VEGF to GAPDH mRNA RT-PCR band density ratios. As with mRNA expression, CA significantly promoted VEGF121 (34 KD), vegf165 (38 kD) and vegf189 (40 KD), but also had the highest effect at 1.0mm, after which the protein expression level was reduced in response to increasing $Ca < sup > 2 + < / sup >$ concentrations. Figure 6 (b) refers to the scatter plot of VEGF to GAPDH protein band density ratios. The promoting effect of Ca ion on VEGF165 protein expression was more obvious than that on VEGF121 and vegf189.

Figure 7 refers to the case of VEGFRs protein expression after Ca ion stimulation. Like the trend of expression levels of mRNA, VEGFR-1,3 protein expression levels reached the highest under the action of 1.0 MMCA ion. Whereas at 0.5 mm CA action, VEGFR-2 reached the peak and remained there at 1.0 MMCA action, after which it gradually returned to the baseline level with the increase of Ca ion concentration.

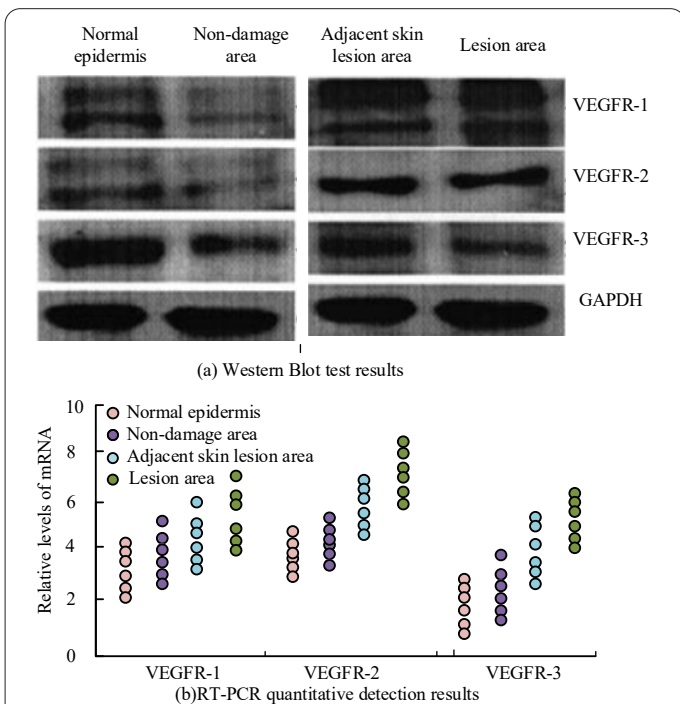


Figure 5. mRNA RT-PCR results of VEGFRs cultured in vivo.

Correlation between VEGFRs protein expression and IOD

To further confirm the relationship between the IOD of psoriasis and VEGFRs' protein expression, figures 8 (a), 8 (b), and 8 (c) refer to the correlation. The findings of the correlation analysis revealed that the correlations of VEGFR-1,2,3 in nonlesional areas of psoriasis were, respectively, 0.546, 0.587, and 0.567 ($P < 0.05$). The correlations were 0.612, 0.632, and 0.625, respectively, in the adjacent lesional area and the three receptors for VEGFRs, and all were significant ($P < 0.05$). The correlations between lesional areas and the three VEGFRs receptors were 0.524, 0.562, and 0.578, respectively ($P < 0.05$).

Figure 9 refers to the correlation between VEGFRs protein expression and normal epidermal IOD. The correlations were 0.521, 0.535, and 0.534, respectively ($P < 0.05$).

Discussion

The incidence of psoriasis is 1% - 3% in European and American populations, whereas, in our 1984 sampling survey, the prevalence of psoriasis was found to be 0.123%, of which, the incidence in the northern region was higher than that in the southern region. Psoriasis is inherited, most dominantly, as a lifelong disease characterized by chronic recurrent exacerbations alternating with exacer-

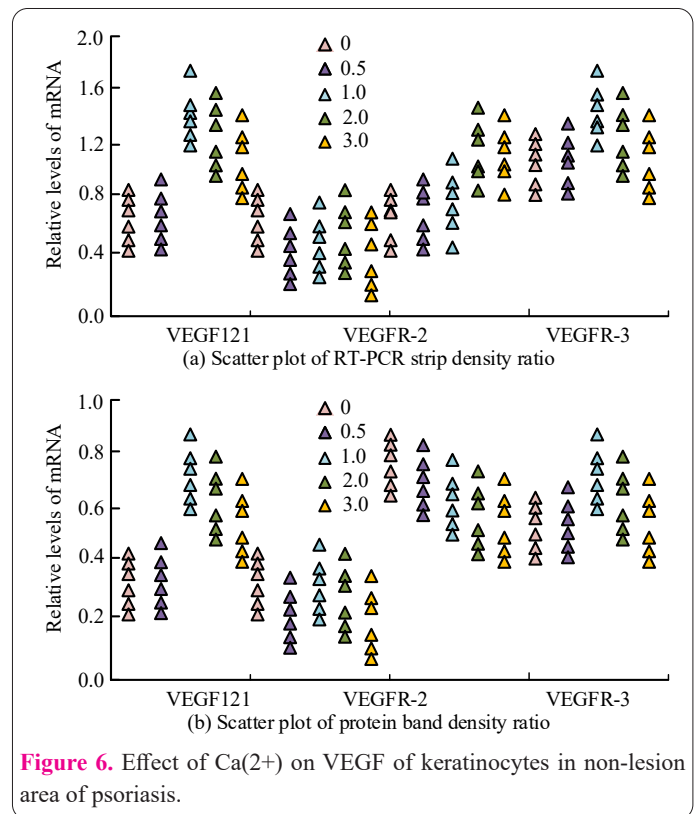


Figure 6. Effect of Ca(2+) on VEGF of keratinocytes in non-lesion area of psoriasis.

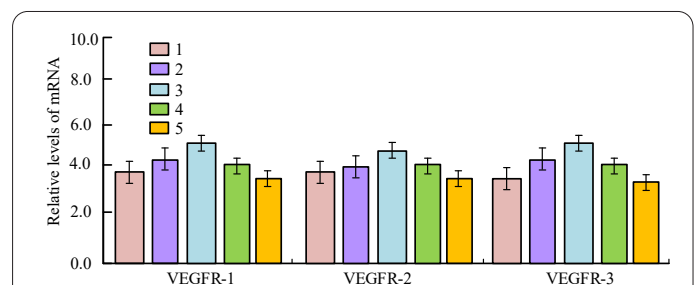


Figure 7. Expression of VEGFRs protein after Ca ion stimulation.

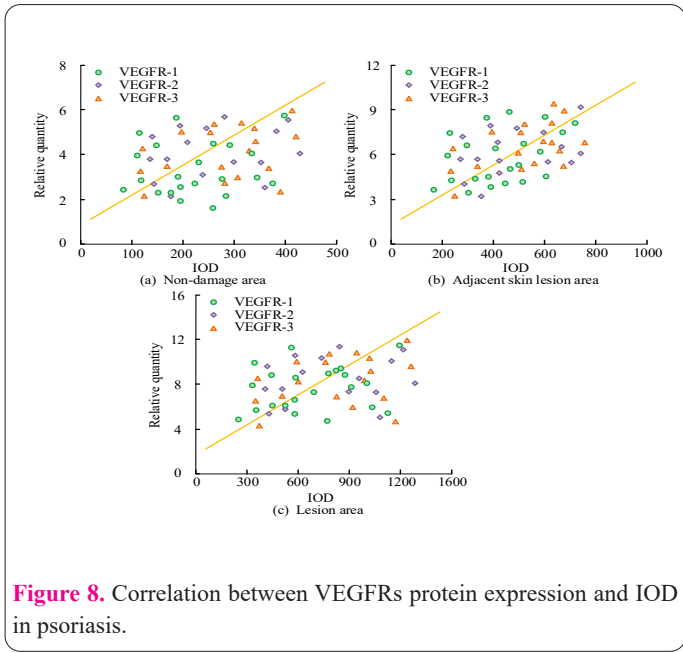


Figure 8. Correlation between VEGFRs protein expression and IOD in psoriasis.

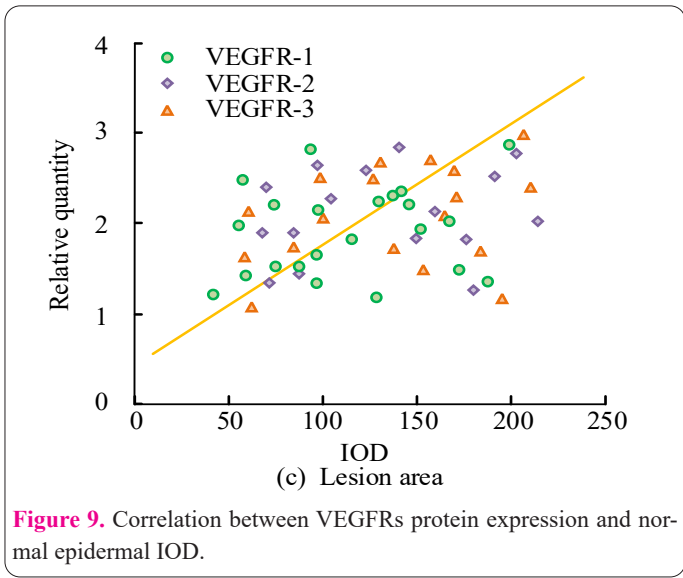


Figure 9. Correlation between VEGFRs protein expression and normal epidermal IOD.

bations and remissions. The underlying psoriatic patients are numerous and only certain environmental factors can initiate the disease. Environmental factors influence the course and severity of the disease, which can vary considerably in extent and severity. There has been an ongoing debate surrounding whether the pathogenesis of psoriasis is caused by a primary epidermal keratinocyte abnormality or an immune system disorder. Alteration of T cell function is typically thought of as a potential etiological factor causing psoriasis, even though these two hypotheses are not mutually exclusive. Yet, it cannot be denied that keratinocytes also possess an important function in the onset and course of psoriasis (7,8). In normal healthy adult, epidermis VEGFR-1,2 are mainly located in the stratum basale as well as the acanthocyte layer adjacent to the basal layer, and in the stratum granulosum as well as the acanthocyte layer adjacent to the stratum granulosum, keratinocytes express little egfr-1 and V2. However, in non-lesional psoriatic areas and adjacent lesional areas, the fluorescent signal of VEGFR-1,2 strongly labeled keratinocytes throughout all the skin's layers besides the stratum corneum, as well as keratinocytes in the epidermal full thickness of psoriatic skin, including cells with parakeratosis of the stratum corneum.

In the skin of patients with psoriasis, fluorescent signals for VEGFR-1,2 are strongly observed on keratinocytes in all layers except nonlesional and adjacent lesional skin of psoriasis and full-thickness epidermal keratinocytes of the lesional area of psoriasis (9-11). The results showed that the distribution of V3 in psoriatic nonlesional and adjacent skin lesions was consistent with normal epidermal distribution, whereas all epidermal layers of psoriatic lesions expressed V3. Studies have shown that simultaneous activation of skin T cells and keratinocyte activator of transcription 3 (STAT3) and a signal transducer is required for the formation of desquamation-induced psoriatic lesions in transgenic mice. The immune system and activated keratinocytes are connected through STAT3. Cells, both of which are interdependent are involved in the pathogenesis of psoriasis (12-14). Uninjured normal skin has a thin epidermis, keratinocytes differentiate into keratinocytes, and keratinocytes become black. And in the papillary layer of the healthy skin dermis, only tiny capillaries are visible. and lymphocyte infiltration is less. Dendritic cells in noninjured areas were also activated by oligonucleotide array analysis. Certain abnormalities also occur in nonlesional skin vessels, with elevated endothelial venules, reduced capillary resistance and reduced endothelial factor expression (15-17). The nonlesional epidermis of psoriasis patients compared with normal epidermis β The number of 1-integrin-expressing cells decreased, β 1-integrin-expressing cells were attenuated in intensity and mostly transiently proliferating. Psoriatic keratinocytes are a major source of proangiogenic factors, including TNF- α , IL-8, transforming growth factor α , Endothelial cells stimulate angiogenic factors, thymidine phosphorylase (TP) and VEGF. Long-term transgenesis of VEGF in the skin results in a complex inflammatory state with cellular and molecular features of human psoriasis, such as hyperplasia and dermal vasculitis, epidermal thickening, abnormal keratinocyte differentiation, and typical inflammatory cell infiltration. For a long time, it was believed that psoriatic redness is due to cutaneous vasodilation, with vascular changes occurring early in psoriasis and increased VEGF levels in lesional skin (18-20). Psoriatic skin vessels are highly abnormal and exhibit increased permeability, leading to features of swollen psoriatic lesions, while expressing markers of vascular inflammation, such as E-selectin, vascular cell adhesion molecule 1, and intercellular adhesion molecule 1. The finding that VEGF-mediated activation of the vascular endothelium plays a central role in the pathogenesis of psoriasis further suggests that the genetic makeup of individual vessels determines susceptibility to this disease. It is important to note, however, that the number of individuals studied is relatively small, and cohort studies with a large number of patients are needed to confirm and further elucidate the genetic makeup of the vasculature in psoriasis.

The mRNA levels of VEGFR-1,2,3 increased gradually, and the mRNA levels of VEGFR in keratinocytes of the epidermis of lesional areas increased gradually. The distribution of V3 distribution between normal and psoriatic epidermis is not significantly different, unlike V1 and V2. V3 is mainly expressed in the lymphatic endothelium in the tissues of adults. Lymphatic endothelium cells undergo apoptosis when V3 signaling is inhibited by soluble VEGFR-3 protein, which also causes lymphatic vessel development to regress. Inhibiting V3 signaling also

greatly reduces corneal dendritic cell trafficking to draining lymph nodes and avoids delayed hypersensitivity and corneal graft rejection, indicating a potential function for V3 in adaptive immunity (21-23). In certain tumors, such as melanoma and breast cancer, VEGFR-3 is activated and its expression is increased. V3 inhibitor could significantly inhibit lymphangiogenesis and lymph node metastasis. V3 is abundantly distributed in vascular endothelial cells throughout the early phases of embryonic growth. Large arteries with luminal abnormalities develop when the V3 gene is disrupted. After organogenesis, V3 is mainly restricted to lymphatic endothelial cells (24-26). Inactivation of V3 by monoclonal antibodies inhibits angiogenesis and tumor tissue growth, so V3 may be necessary for maintaining endothelial cell integrity during angiogenesis. V3 can also maintain vascular integrity by regulating the V2 signaling pathway. More research is, therefore, necessary to determine the importance of VEGFR-3 expression within the epidermis, as well as its correlation to the biological activity of epidermal keratinocytes.

Ca ions enhanced VEGFR-1,2,3 mRNA and protein expression in keratinocytes of nonlesional areas of psoriasis. The protein expression of VEGFRs was positively correlated with the IOD value in the psoriatic cortex and normal subjects. Studies conducted *in vitro* have demonstrated that calcium ions have a role in mediating epidermal keratinocyte growth. An increase in free Ca ions following an increase in extracellular Ca ions may be one of the prerequisites for keratinocyte differentiation. Calmodulin levels are 2-3 times higher in psoriatic plaque areas than in normal skin, and they are also significantly higher in psoriatic skin nearby affected areas (27-30). In addition, Ca ions are involved in mediating the expression of VEGF. Vegf2 and VEGF165 expression increased during the differentiation of retinal pigment epithelial cells induced by calcium ions. VEGF expression is inhibited by the Ca channel antagonist benidipine, and epidermal keratinocytes are the main source cells of VEGF. Thus, in non-lesional psoriasis cells, the effects of Ca ions on VEGF isoform expression and the effects of Ca and VEGF165 on VEGFR expression were experimentally studied. To investigate the potential factors contributing to the high expression of VEGFRs in psoriasis. The serum level of VEGF was significantly increased in severe psoriasis patients, and the level of VEGF was directly correlated with disease activity. However, the exact mechanism by which Ca ions and VEGF promote VEGFRs expression was not discovered during the experiment. The survival of psoriatic keratinocytes may be significantly influenced by the autocrine loop. Bevacizumab modestly or significantly reduced VEGF-induced upregulation of VEGFR in nonlesional psoriatic keratinocytes, but bevacizumab did not prevent CA-induced upregulation of VEGFR expression. Based on these results, the experiments allowed the following two conclusions: Independent of VEGF, CA increased the expression of VEGFRs. Moreover, the amount of VEGF produced by Ca was insufficient to control the expression of VEGFRs.

In vivo and *in vitro* investigations have revealed upregulation of VEGFR-1,2,3 in keratinocytes of the psoriatic epidermis. Experiments have also demonstrated that exogenous VEGF1ss and Ca ions can enhance VEGFRs expression in keratinocytes of non-lesional skin of psoriasis. Although Ca ions also increased the expression of the VEGF isoforms VEGF121, VEGF189, and particular-

ly VEGF165 at the mRNA and protein levels, inhibiting VEGF activity with a VEGF-specific neutralizing antibody did not prevent Ca ions from inducing an increase in the levels of the VEGFR proteins. Ca ions may so directly encourage the development of VEGFRs without the involvement of VEGF. The follow-up studies about VEGF / VEGFRs need to be continued, which will provide more valuable clues and thus provide new molecular targets for psoriasis treatment, and monoclonal antibodies against VEGFRs will be one of the important targets for psoriasis treatment in the future.

Funding

The research is supported by: Science and Technology Project of Jiangxi Provincial Department of Education in 2019 (No.: GJJ190853); Science and Technology Plan Project of Jiangxi Provincial Health Commission in 2022 (No.: 202212674).

References

1. Luengas-Martinez A, Hardman-Smart J, Paus R, Young HS. Vascular endothelial growth factor-A as a promising therapeutic target for the management of psoriasis. *Exp Dermatol* 2020 Aug; 29(8): 687-698. <https://doi.org/10.1111/exd.14151>
2. Young HS, Kamaly-Asl ID, Laws PM, Pemberton P, Griffiths CE. Genetic interaction between placental growth factor and vascular endothelial growth factor A in psoriasis. *Clin Exp Dermatol* 2020 Apr 1; 45(3): 302-308.
3. Luengas-Martinez A, Paus R, Young HS. Antivascular endothelial growth factor-A therapy: a novel personalized treatment approach for psoriasis. *Br J Dermatol* 2022 May 1; 186(5): 782-791. <https://doi.org/10.1111/bjd.20940>
4. Li J, Hou H, Zhou L, Wang J, Liang J, Li J, Hou R, Niu X, Yin G, Li X, Zhang K. Increased angiogenesis and migration of dermal microvascular endothelial cells from patients with psoriasis. *Exp Dermatol* 2021 Jul; 30(7): 973-981. <https://doi.org/10.1111/exd.14329>
5. Sally R, Ugonabo N, Nguyen A, Kim RH, Sicco KL. Lenvatinib-induced psoriasiform eruption and palmoplantar erythema in a patient with hepatocellular carcinoma. *JAAD Case Rep* 2021 Sep 1; 15: 1-3. <https://doi.org/10.1016/j.jcdr.2021.07.001>
6. Boda D, Dehelean C. Immuno-dermatological processes involved in chronic skin diseases: Highlights of the Second Conference of the Romanian Society for Immuno-Dermatology, Bucharest, September, 2018. *Exp Ther Med* 2019 Aug 1; 18(2): 873-874. <https://doi.org/10.3892/etm.2019.7690>
7. Alsohaimi A. The pathogenic role of vascular endothelial growth factor (VEGF) in skin diseases. *Adv Med Med Res* 2019 Nov 25; 2(1): 27-37.
8. Xue Y, Liu Y, Bian X, Zhang Y, Li Y, Zhang Q, Yin M. miR-205-5p inhibits psoriasis-associated proliferation and angiogenesis: Wnt/ β -catenin and mitogen-activated protein kinase signaling pathway are involved. *J Dermatol* 2020 Aug; 47(8): 882-892. <https://doi.org/10.1111/1346-8138.15370>
9. Adachi H, Nosaka C, Atsumi S, Nakae K, Umezawa Y, Sawa R, Kubota Y, Nakane C, Shibuya M, Nishimura Y. Structure-activity relationships of natural quinone vegfrecine analogs with potent activity against VEGFR-1 and-2 tyrosine kinases. *J Antibiot* 2021 Oct; 74(10): 734-742. <https://doi.org/10.1038/s41429-021-00445-y>
10. Gu H, Zhang Y, Zeng W, Xia Y. Participation of interferons in psoriatic inflammation. *Cytokine Growth Factor Rev* 2022 Apr 1; 64: 12-20. <https://doi.org/10.1016/j.cytogfr.2021.12.002>

11. Samotij D, Nedoszytko B, Bartosińska J, Batorycka-Baran A, Czajkowski R, Dobrucki I, Dobrucki L, Górecka-Sokołowska M, Janaszak-Jasienicka A, Krasowska D, Kalinowski L. Pathogenesis of psoriasis in the “omic” era. Part I. Epidemiology, clinical manifestation, immunological and neuroendocrine disturbances. *Postepy Dermatol Alergol* 2020 Apr 1; 37(2): 135-153.
12. Lien JC, Chung CL, Huang TF, Chang TC, Chen KC, Gao GY, Hsu MJ, Huang SW. A novel 2-aminobenzimidazole-based compound Jzu 17 exhibits anti-angiogenesis effects by targeting VEGFR-2 signalling. *Br J Pharmacol* 2019 Oct; 176(20): 4034-4049. <https://doi.org/10.1111/bph.14813>
13. Jaballah MY, Serya RA, Saad N, Khojah SM, Ahmed M, Barakat K, Abouzid KA. Towards discovery of novel scaffold with potent antiangiogenic activity; design, synthesis of pyridazine based compounds, impact of hinge interaction, and accessibility of their bioactive conformation on VEGFR-2 activities. *J Enzyme Inhib Med Chem* 2019 Jan 1; 34(1): 1573-1589. <https://doi.org/10.1080/14756366.2019.1651723>
14. Qiu S, Shi C, Anbazhagan AN, Das V, Arora V, Kc R, Li X, O-Sullivan I, van Wijnen A, Chintharlapalli S, Gott-Velis G. Absence of VEGFR-1/Flt-1 signaling pathway in mice results in insensitivity to discogenic low back pain in an established disc injury mouse model. *J Cell Physiol* 2020 Jun; 235(6): 5305-5317. <https://doi.org/10.1002/jcp.29416>
15. Pan X, Liang L, Si RU, Wang J, Zhang Q, Zhou H, Zhang L, Zhang J. Discovery of novel anti-angiogenesis agents. Part 10: Multi-target inhibitors of VEGFR-2, Tie-2 and EphB4 incorporated with 1, 2, 3-triazol. *Eur J Med Chem* 2019 Feb 1; 163: 1-9. <https://doi.org/10.1016/j.ejmech.2018.11.042>
16. Momen Razmgah M, Ghahremanloo A, Javid H, AlAlikhhan A, Afshari AR, Hashemy SI. The effect of substance P and its specific antagonist (aprepitant) on the expression of MMP-2, MMP-9, VEGF, and VEGFR in ovarian cancer cells. *Mol Biol Rep* 2022 Oct; 49(10): 9307-9314. <https://doi.org/10.1007/s11033-022-07771-w>
17. Oplawski M, Dziobek K, Zmarzły N, Grabarek B, Halski T, Januszyk P, Kuś-Kierach A, Adwent I, Dąbrus D, Kielbasiński K, Boroń D. Expression profile of VEGF-C, VEGF-D, and VEGFR-3 in different grades of endometrial cancer. *Curr Pharm Biotechnol* 2019 Oct 1; 20(12): 1004-1010. <https://doi.org/10.2174/1389201020666190718164431>
18. Abdulazeem L, Tariq A, Jasim SA. An investigation of vascular endothelial growth factor (VEGFR-1 and VEGFR-2) in burn wound healing. *Arch Razi Inst* 2022 Apr 30; 77(2): 747-751. <https://doi.org/10.22092/ari.2022.356981.1954>
19. Luan B, Yuan R, Xin QQ, Cong WH, Song P. Effects of components in stasis-resolving and collateral-dredging Chinese herbal medicines on angiogenesis and inflammatory response of human umbilical vein endothelial cells induced by VEGF. *Zhongguo Zhong Yao Za Zhi* 2022 Feb 1; 47(3): 737-744. <https://doi.org/10.19540/j.cnki.cjcm.20211012.401>
20. Vastarella M, Fabbrocini G, Sibaud V. Hyperkeratotic skin adverse events induced by anticancer treatments: a comprehensive review. *Drug Saf* 2020 May; 43(5): 395-408. <https://doi.org/10.1007/s40264-020-00907-6>
21. Rapalli VK, Waghule T, Gorantla S, Dubey SK, Saha RN, Singhvi G. Psoriasis: pathological mechanisms, current pharmacological therapies, and emerging drug delivery systems. *Drug Discov Today* 2020 Dec 1; 25(12): 2212-2226.
22. Luengas-Martinez A, Paus R, Iqbal M, Bailey L, Ray DW, Young HS. Circadian rhythms in psoriasis and the potential of chronotherapy in psoriasis management. *Exp Dermatol* 2022 Nov; 31(11): 1800-1809. <https://doi.org/10.1111/exd.14649>
23. Iwasaki K, Uno Y, Utoh M, Yamazaki H. Importance of cynomolgus monkeys in development of monoclonal antibody drugs. *Drug Metab Pharmacokinet* 2019 Feb 1; 34(1): 55-63. <https://doi.org/10.1016/j.dmpk.2018.02.003>
24. King R, Tanna N, Patel V. Medication-related osteonecrosis of the jaw unrelated to bisphosphonates and denosumab—a review. *Oral Surg Oral Med Oral Pathol Oral Radiol* 2019 Apr 1; 127(4): 289-299. <https://doi.org/10.1016/j.oooo.2018.11.012>
- Shirani M, Banaii Boroujeni J, Keshavarz S, Karimi M. The Effect of Eight Weeks Aerobic Training Alone or Combined with Grape Seed Extract Supplementation on the Myocardial Expression of VEGF and VEGFR-2 in the Streptozotocin-induced Diabetic Rats. *J Anim Biol* 2022 Aug 23; 14(4): 225-235. <https://doi.org/10.22034/ascij.2022.1938778.1292>
- Ortins-Pina A, Soares-de-Almeida L, Caroli U, Held L, Kempter W, Rütten A, Mentzel T, Kutzner H. Pruriginiform angiomas: reactive angioproliferation in the skin and vascular endothelial growth factors. *Am J Dermatopathol* 2020 Jan 1; 42(1): 29-34. <https://doi.org/10.1097/DAD.0000000000001452>
- Hayran Y, Lay I, Mocan MC, Bozduman T, Ersoy-Evans S. Vascular endothelial growth factor gene polymorphisms in patients with rosacea: A case-control study. *J Am Acad Dermatol* 2019 Aug 1; 81(2): 348-354. <https://doi.org/10.1016/j.jaad.2019.03.055>
- Boki H, Kimura T, Miyagaki T, Suga H, Blauvelt A, Okochi H, Sugaya M, Sato S. Lymphatic dysfunction exacerbates cutaneous tumorigenesis and psoriasis-like skin inflammation through accumulation of inflammatory cytokines. *J Invest Dermatol* 2022 Jun 1; 142(6): 1692-1702. <https://doi.org/10.1016/j.jid.2021.05.039>
- Vranova M, Friess MC, Haghayegh Jahromi N, Collado-Diaz V, Val-lone A, Hagedorn O, Jadhav M, Willrodt AH, Polomska A, Leroux JC, Proulx ST. Opposing roles of endothelial and leukocyte-expressed IL-7R α in the regulation of psoriasis-like skin inflammation. *Sci rep* 2019 Aug 12; 9(1): 11714. <https://doi.org/10.1038/s41598-019-48046-y>.
- Liu L, Sun XY, Lu Y, Song JK, Xing M, Chen X, Luo Y, Ru Y, Chen ST, Li HJ, Li B. Fire needle therapy for the treatment of psoriasis: a quantitative evidence synthesis. *J Altern Complement Med* 2021 Jan 1; 27(1): 24-37. <https://doi.org/10.1089/acm.2019.0409>. Epub 2020 Jul 31.